

Photon radiation effects in kinematic reconstruction of top quarks

D. Dobur, J. Knolle, G. Mestdach and K. Skovpen¹

*Ghent University,
Sint-Pietersnieuwstraat 33, 9000 Gent*

E-mail: kirill.skovpen@cern.ch

ABSTRACT: Kinematic reconstruction of top quarks allows to define a set of kinematic observables relevant to various physics processes that involve top quarks and provides an additional handle for the suppression of background events. Radiation of photons in association with the top quarks alters the kinematics and the topology of the event, leading to visible systematic effects in measurable observables. The present study introduces an improved reconstruction of the top quark kinematics in the presence of photon radiation. The results are presented for processes with top quark pair production, as well as for singly-produced top quarks.

¹Corresponding author.

Contents

1	Introduction	2
2	Photon radiation in processes with top quarks	3
3	Kinematic event reconstruction	4
4	Results	7
5	Summary	8

1 Introduction

The measurement of the top quark production cross sections, as well as the study of the properties of top quarks, remain a foreground direction in a large number of experimental studies across several experiments at the Large Hadron Collider (LHC) at CERN. Top quarks are copiously produced at the LHC, allowing to achieve an unprecedented precision in the measurement of the inclusive production cross sections of top quark pairs ($t\bar{t}$) down to the level of $\simeq 2\%$ [1]. The production cross section of a single top quark ($t(\bar{t})$) in the predominant t channel has been measured with the precision of $\simeq 15\%$ [2]. In addition to the measurement of the inclusive cross sections, the amount of recorded data at the LHC allows to perform measurements of the differential production cross sections as a function of various kinematic observables.

The electroweak couplings of the top quark can be directly probed in processes involving the associated production of top quarks with vector bosons. The production of top quarks in association with a photon ($t\bar{t}\gamma$) provides direct access to the study of the electromagnetic couplings of the top quark at hadron colliders [3–8]. With respect to $t\bar{t}$ production, the top quark charge asymmetry is particularly enhanced to the level of $\simeq 10\%$ in the $q\bar{q}$ -initiated production channel of the $t\bar{t}\gamma$ process [9], which is significantly larger than in $t\bar{t}$. Potential new physics effects can be induced as anomalous electric dipole moments, modifying the standard model (SM) predictions for various kinematic observables for this process [10, 11]. Within the effective field theory (EFT) approach, the potential modifications of the structure of the $t\bar{t}\gamma$ interaction vertex are parametrized with the respective dimension-six operators [12].

The $t\bar{t}\gamma$ process was experimentally studied at CDF [13], ATLAS [14–17] and CMS [18, 19]. The measured cross sections in semileptonic and dilepton channels show good agreement with the SM predictions. The differential cross section is measured as a function of multiple kinematic variables involving leptons and radiated photons. Several of these variables, such as the angular separation between the two leptons, which can be reconstructed in the dilepton channel, are particularly sensitive to $t\bar{t}$ spin correlation effects. The charge asymmetry has not yet been studied experimentally, as it requires a good handle to separate the gg - and $q\bar{q}$ -initiated $t\bar{t}\gamma$ production processes [9]. It was shown that the photon rapidity can potentially allow to distinguish between these two processes in the measured differential distributions. The measurement of the $t\bar{t}$ charge asymmetry in $t\bar{t}\gamma$ events however requires a full reconstruction of the $t\bar{t}\gamma$ final state, which has not yet been established in experimental studies.

In addition to the $t\bar{t}$ process, the photons can also be radiated in processes involving the production of single top quarks, $t(\bar{t})\gamma$ [20, 21]. This process has been studied by the CMS experiment leading to the observed evidence of 4.4 standard deviations [22]. The production mechanism of $t(\bar{t})\gamma$ is dominated by the electroweak t channel process, where the light-flavour quark in the hard-scattering process recoils against the top quark to produce an energetic jet in the forward region of the detector. As in $t\bar{t}\gamma$ production, the $t(\bar{t})\gamma$ process is sensitive to the electromagnetic dipole moments of the top quark and potential new physics effects described within an EFT approach.

2 Photon radiation in processes with top quarks

The performed study aims at reconstructing top quarks in the presence of photon radiation in several event topologies including single-top and $t\bar{t}$ production channels. The photon can be emitted from any charged particle that is involved in the process, from the products of subsequent decays of unstable particles, as well as in the parton shower process. The proposed algorithm of the kinematic reconstruction targets at properly assigning the origin of the emitted photon. The study primarily focuses on the processes with the production of top quarks, where a photon is radiated at the matrix-element (ME) level. The photon can be radiated from the initial state quarks, the intermediate top quarks and W bosons, as well as from the final-state quarks and leptons. The kinematic effects that are induced by the photon radiation in the $t\bar{t}$ process were previously discussed in Ref. [5], indicating a significant fraction of events with photon emission from top quark decays, especially in the low photon p_T region. The inclusion of radiated photons in the reconstruction of events with top quarks is therefore crucial in order to properly define the top quark-related kinematic observables at the reconstruction level in the measurement of differential cross sections, as well as in studies of the $t\bar{t}$ charge asymmetry and spin correlation effects.

Leptonic decays of W bosons originating from top quark decays lead to the presence of a neutrino (or an anti-neutrino) in events, which can only be partially reconstructed at hadron colliders. The longitudinal component of the neutrino's momentum (p_z^ν) remains unconstrained. However, it can be inferred by imposing a set of kinematic constraints on the topology of the reconstructed events that describe the top quark decay kinematics. The p_z^ν can be derived by resolving a quadratic equation involving constraints on the reconstructed masses of the W boson and the top quark. The W boson mass is reconstructed from a lepton and a neutrino ($W^- \rightarrow \ell^- \bar{\nu}$, $W^+ \rightarrow \ell^+ \nu$), while the reconstruction of the top quark mass additionally involves the hadronic jet that is associated with the decay of a heavy hadron, a b jet ($t \rightarrow \ell^+ \nu b$, $\bar{t} \rightarrow \ell^- \bar{\nu} \bar{b}$). The missing transverse energy, (E_T^{miss}) which is defined as the negative vectorial sum of all reconstructed objects in the event in the transverse plane of the colliding beams, provides crucial information about the transverse component of the neutrino's momentum. In the case of the fully hadronic decays of the top quarks, the reconstruction of the top quark mass involves three jets, one of which is identified as a b jet. The dominant contribution to the measured experimental resolution in the reconstructed spectra of the W boson and the top quark masses is therefore predominantly described by the jet energy scale and resolution effects. The production of single top quarks leads to the presence of either a leptonic or a hadronic W boson decay, with an additional b quark arising from the top quark decay.

The top quarks that are produced in pairs lead to two distinctive event topologies. The semileptonic $t\bar{t}$ events contain one leptonic decay of a W boson, with the other W boson decaying hadronically. The dilepton final states arise from leptonic decays of two W bosons, subsequently producing two neutrinos in the final state. The kinematic properties of the described event topologies can be fully established, if the corresponding leptons, jets and E_T^{miss} are well reconstructed in the event.

The kinematic reconstruction of top quarks is performed in $t\bar{t}\gamma$ semileptonic and dilepton events, as well as in events with an associative production of single top quarks and a photon with leptonic W boson decays. Events are simulated with the MadGraph5_aMC@NLO v2.8.2 [23]

generator at leading order, interfaced with the Pythia v8.1 [24] program for the simulation of hadronization and fragmentation processes. At ME level, the event generation corresponds to $2 \rightarrow 7$ and $2 \rightarrow 5$ production processes for $t\bar{t}\gamma$ and $t(\bar{t})\gamma$, respectively, where a photon can be radiated from any charged particle involved in the process. Event generation involves on-shell top quarks, and it accounts for interference effects in the relevant production diagrams. The photon origin is determined by looking at its ancestors in the generated event record. Angular separation between a photon with a minimum p_T of 5 GeV and any other final-state particle is required to be $\Delta R = \sqrt{(\Delta\phi)^2 + (\Delta\eta)^2} > 0.3$. The generated events are passed through a simplified detector simulation that is realized within the Delphes v.3.4.2 [25] package that models a realistic detector response and performs the event reconstruction. Reconstructed events that correspond to at least one top quark decaying via a leptonically decaying W boson are required to have at least one lepton (electron or muon) and one photon with $p_T > 20$ GeV and an absolute pseudorapidity, $|\eta|$, of less than 2.4. Jets are reconstructed using the anti- k_T jet algorithm [26] with $R = 0.4$ and are selected with $p_T > 30$ GeV and $|\eta| < 2.4$. It is additionally required that jets do not have a nearby lepton that is reconstructed within $\Delta R = 0.4$. The photon must be separated from any lepton or jet object by $\Delta R > 0.4$. The event selection applied in the dilepton channel requires the presence of at least two leptons in the final state. The E_T^{miss} is reconstructed from tracks and particle-flow calorimeter deposits. The reconstructed leptons, jets and the photon, are geometrically matched within $\Delta R = 0.4$ to the corresponding generated particles that are associated with the parton-level production and decay processes. Selected events where all generated particles are properly matched to the corresponding reconstructed objects are used to perform the study of the kinematic reconstruction.

3 Kinematic event reconstruction

Events that satisfy the described selection criteria are used to perform a kinematic reconstruction of the $t\bar{t}\gamma$ and $t(\bar{t})\gamma$ processes, and are classified into event categories where the photon is radiated either from the production part of the parton-level process (“production”), or from the decay products of top quarks (“decay”). The number of reconstructed objects used as input to the kinematic fit corresponds to the number of generated particles at the ME level. The fraction of the events where a photon is emitted in the decay, and the distributions representing an angular separation between the photon and the closest parton-level final state particle, are presented in Fig. 1. The radiation of photons with high momentum is kinematically enhanced in the production case, while the emitted photons in the top quark decay are mainly radiated at small angles and generally have a softer p_T spectrum. The observed difference in the measured event fractions between the semileptonic and the dilepton channels is due to the selection criteria applied on the ΔR separation between a reconstructed photon and other final-state objects.

The reconstruction of the neutrino’s longitudinal momentum in the context of $t\bar{t}$ events, covering both the semileptonic and the dilepton final states, is discussed in detail in Refs. [27–35], with the analytic solutions for p_z^ν derived in Refs. [36–38]. The methodology of the presented study does not directly use the proposed analytic solutions, but rather attempts at resolving the system of the relevant unknowns by performing a likelihood fit based on the initial set of equations involving p_z^ν . A suitable solution for p_z^ν is determined in a log-likelihood fit that is implemented in a dedicated TopPhi t package [39], which makes use of the ROOT toolkit libraries [40]. The fit is based on

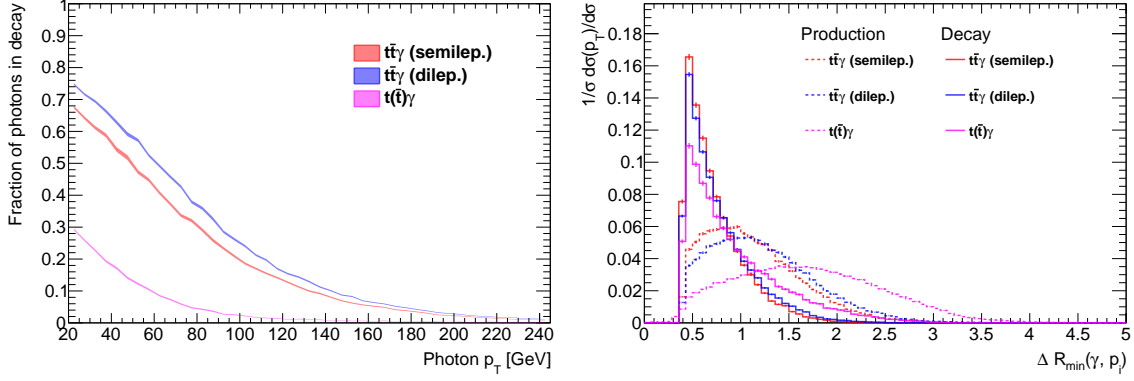


Figure 1. Left: Relative fraction of events with a photon that is radiated from the decay products of top quarks. Right: Minimal ΔR separation between the photon and any of the parton-level final state particles.

the comparison of the reconstructed top quark and the W boson masses with the corresponding truth-level values. The general likelihood function that is used to perform a fit is defined as:

$$\mathcal{L} = -2\ln \left[\prod_i P_i(\text{rec}|\text{gen}) \times P_{\text{neg}} \right], \quad (3.1)$$

where the P_i denote the probabilities of the reconstructed masses of a top quark and a W boson to correspond to their predicted values from generator, following the Breit-Wigner distribution.

The likelihood function contains four main terms that correspond to the top quark, the top antiquark, and two W bosons in the kinematic reconstruction of $t\bar{t}\gamma$ events. There is a single neutrino produced in semileptonic $t\bar{t}\gamma$ events, and therefore the p_z^ν remains the only unknown. As a consequence of resolving a quadratic equation, there are two possible p_z^ν solutions. The ambiguity is resolved by imposing a constraint on the reconstructed top quark mass value, in addition to the W boson mass requirement. The hadronic decay of the top quark in $t\bar{t}\gamma$ semileptonic events is reconstructed using the corresponding W boson and top quark mass requirements, leading to four constraints, together with the reconstruction of the leptonic top quark decay. There are also four main likelihood terms included in the kinematic fit of dileptonic $t\bar{t}\gamma$ events. However, in this case there are two neutrinos with four unknowns in the reconstruction. With four terms corresponding to the W boson and top quark masses included in the likelihood fit, the minimized function has zero degrees of freedom in the fit. There are two likelihood terms that are included in the $t(\bar{t})\gamma$ case, similar to the reconstruction of the leptonic decay of the top quark in the $t\bar{t}\gamma$ semileptonic system. The last term (P_{neg}) in the likelihood definition refers to the additional penalty term against the nonphysical solutions associated with imaginary values that can appear in the derivation of the neutrino's longitudinal momentum. This penalty term is defined as the sum of absolute values of square roots giving imaginary solutions in event, guiding the minimization procedure towards the correct minima.

The likelihood function is evaluated for each possible assignment of reconstructed leptons and jets to the hard-process particles. The likelihood minimization is performed in each permutation of selected leptons, jets and photons in event. The permutations include the photon's origin assignment to various particles involved in the hard process. In order to account for possible resolution effects

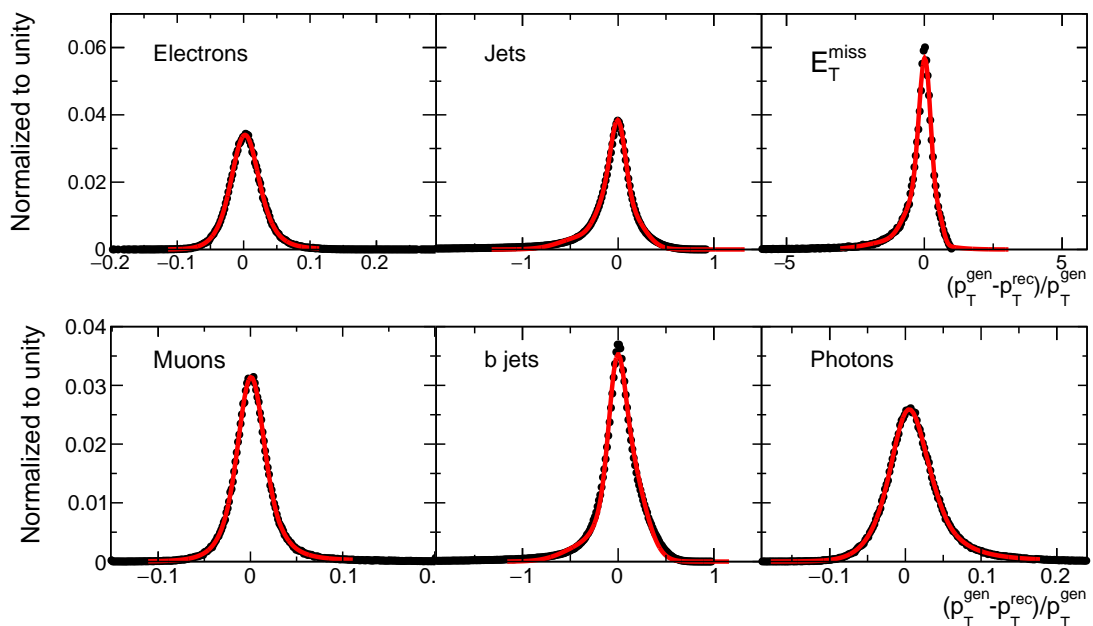


Figure 2. Some examples of transfer functions used in the kinematic reconstruction that are measured for various reconstructed objects.

in the reconstruction process, a set of the so-called transfer functions (TFs) is used that establishes the correspondence between the generated particles and their reconstructed counterparts. A TF is defined as the relative difference between the truth-level and the reconstructed quantities, measured in each considered category of the reconstructed objects, including jets, E_T^{miss} , leptons and photons, as presented in Fig. 2. The use of TFs maximizes the probability of finding a viable solution for p_z^ν . The TFs are used as probability density functions to perform the generation of pseudo-experiments in each event to define the four-momenta of reconstructed objects, and in each of these variations the corresponding likelihood value is computed. Typically, about 100 iterations are needed to find the correct minimum in events containing one neutrino. The kinematic fit in dilepton $t\bar{t}\gamma$ events uses the same minimization algorithm involving TFs with an additional minimization step performed in MINUIT [41]. This is done in order to improve the convergence of the minimization process when dealing with the more complex two-neutrino case of dilepton events. The system of equations used to derive the solution for p_z^ν can be resolved in all relevant event topologies with an efficiency close to 100%, with some dependence on the number of pseudo-experiments. Permutation that gives the minimum value of the log-likelihood function is selected to correspond to the best assignment of reconstructed leptons, jets and photons, to particles generated at parton level. The fitted values of the likelihood are shown in Fig. 3. As described above, the minimum value of the likelihood is close to zero in $\approx 99\%$ of selected events in the dilepton case, because the performed fit has no degrees of freedom. The corresponding results in $t\bar{t}\gamma$ semileptonic events tend to diverge from zero because the relevant system of equations is overconstrained in the fit.

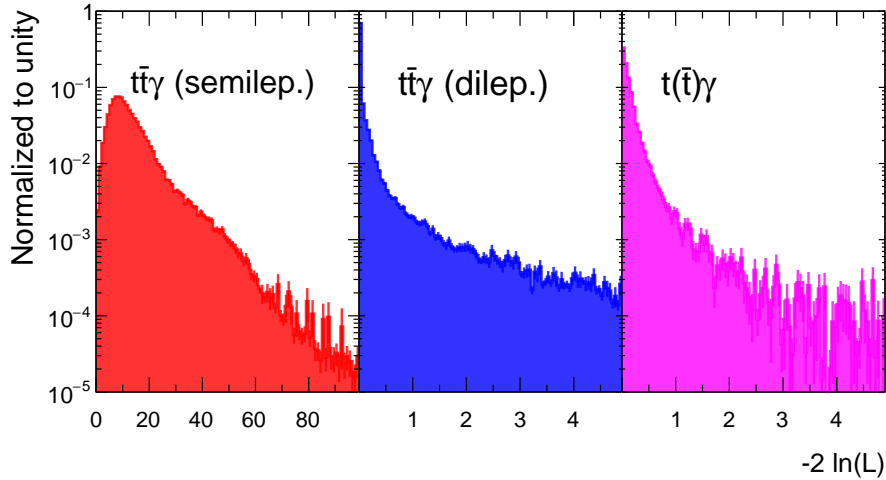


Figure 3. Minimum value of the log-likelihood function used in the kinematic fit in $t\bar{t}\gamma$ semileptonic (left), $t\bar{t}\gamma$ dilepton (middle) and $t(\bar{t})\gamma$ (right) events.

4 Results

The performance of the proposed method is studied by measuring the efficiency of the correct assignment of reconstructed objects to generated leptons, quarks and photons. In order to avoid accounting for any inefficiencies due to event reconstruction effects, the selected events must have the parton-level particles matched within $\Delta R = 0.4$ to the corresponding reconstructed objects. The measured efficiencies are presented in Fig. 4 and correspond to the correct matching between the truth-level generated particles from the decays of top quarks and the reconstructed objects (“top-match”), as well as when all generated parton-level final state particles (leptons, quarks and photons) are correctly matched (“all-match”).

The reconstructed photon in $t\bar{t}$ events can be assigned to either the top quark or a W boson decay, or to any other particle not involved in the top quark decay process. Since there are two top quarks and two W bosons produced in $t\bar{t}$ events, there are four categories in total corresponding to the photon origin in top quark decay chain. The fifth category represents the photon radiation from any charged particle involved in the process, excluding the top quark decay products. A photon is radiated in “decay”, if it is assigned to a top quark or a W boson decay. It is considered as radiation in “production”, otherwise.

The kinematic event reconstruction represents the main handle on the identification of the photon origin in the photon p_T range below $\simeq 200$ GeV. At higher energies, the photon is predominantly emitted in production, consistent with the results obtained from the kinematic fit.

When a photon is radiated in production, the top-match efficiency reaches the values of $\simeq 90\%$ and $\simeq 83\%$ in the semileptonic and dilepton $t\bar{t}\gamma$ production channels, respectively, and is rather stable with respect to the photon p_T . In the case of $t(\bar{t})\gamma$ process, the light-flavour quark-jet is included in the jet-parton permutations when assigning the b-quark jet to the corresponding generator b quark. There is no kinematic requirement that is used in the fit for the recoiling jet

in the $t(\bar{t})\gamma$ process, which leads to a lower b-quark matching efficiency. In the $t\bar{t}\gamma$ semileptonic events the light-flavour quark-jets are used in the calculation of the top quark mass in hadronic W decays, therefore constraining the allowed parameter phase space of the b-quark jet kinematics. When additionally requiring the photon to be correctly assigned to the corresponding hard-process particle, the overall matching efficiency is found to be $\simeq 65\%$ in the region of the low photon p_T in $t\bar{t}\gamma$ semileptonic and $t(\bar{t})\gamma$ events, while it reaches $\simeq 50\%$ in the $t\bar{t}\gamma$ dilepton channel. The kinematic reconstruction in the presence of two neutrinos is associated with larger systematic effects arising from E_T^{miss} and jet reconstruction, with respect to the final states involving a single neutrino. Therefore, the measured matching efficiencies for the reconstructed photon are generally smaller in the $t\bar{t}\gamma$ dilepton channel than in other considered event topologies. At higher values of the photon p_T , the matching efficiency reaches a plateau around 100 GeV, because the photon emission from production becomes dominant, with only a small contribution from the photon arising from the top quark decay.

In the case of photon radiation from the top quark decay, the measured top-match and the all-match efficiencies increase with the photon p_T . The effect of including a radiated photon in the kinematic reconstruction becomes increasingly pronounced at higher values of the photon p_T , where the experimental energy resolution effects in the object reconstruction become less important. The probability to select a permutation that corresponds to the proper matching of all hard-process particles is $\simeq 45\%$ in $t\bar{t}\gamma$ semileptonic events, while it reaches $\simeq 30\%$ and $\simeq 40\%$ in $t\bar{t}\gamma$ dilepton and $t(\bar{t})\gamma$ events, respectively. In case of the hadronic decay of a W boson, the reconstructed jets are allowed to be matched to either of the two quarks from the W boson decay, but not to the same one.

A correct assignment of reconstructed objects to the hard-process particles allows to define kinematic properties of produced top quarks. The comparison between the reconstructed and the generated top quark p_T in $t\bar{t}\gamma$ semileptonic events is presented in Fig. 5. A similar comparison for an hadronically decaying top quark is shown in Fig. 6. The results from the application of kinematic reconstruction to the $t\bar{t}\gamma$ dilepton and $t(\bar{t})\gamma$ events are presented in Figs. 7 and 8, respectively. The comparisons are shown for the case, where the photon is omitted in the kinematic event reconstruction, as well as for the case where it is included in the fit. When the photon is not accounted for in the reconstruction, the correlation between the reconstructed and generated top quark p_T appears to be clearly biased and correlated to the minimum photon p_T requirement that is applied in selected events, while the inclusion of the photon leads to a significantly improved resolution in derived kinematic variables. The results are also presented as the mean values and the corresponding variances in the measured top quark p_T in Fig. 9.

5 Summary

A method for the reconstruction of the top quark event kinematics in the presence of photon radiation is presented. The kinematic reconstruction is applied to events with the production of top quark pairs in association with a photon, and to events with an associated production of single top quarks with a photon. The inclusion of a radiated photon in a kinematic fit allows to significantly improve the precision of reconstructed top quark kinematic observables, when compared to the event generator truth-level information. The proposed method can be used in experimental studies of the processes with top quarks with an additional radiation of photons. It aims at improving the

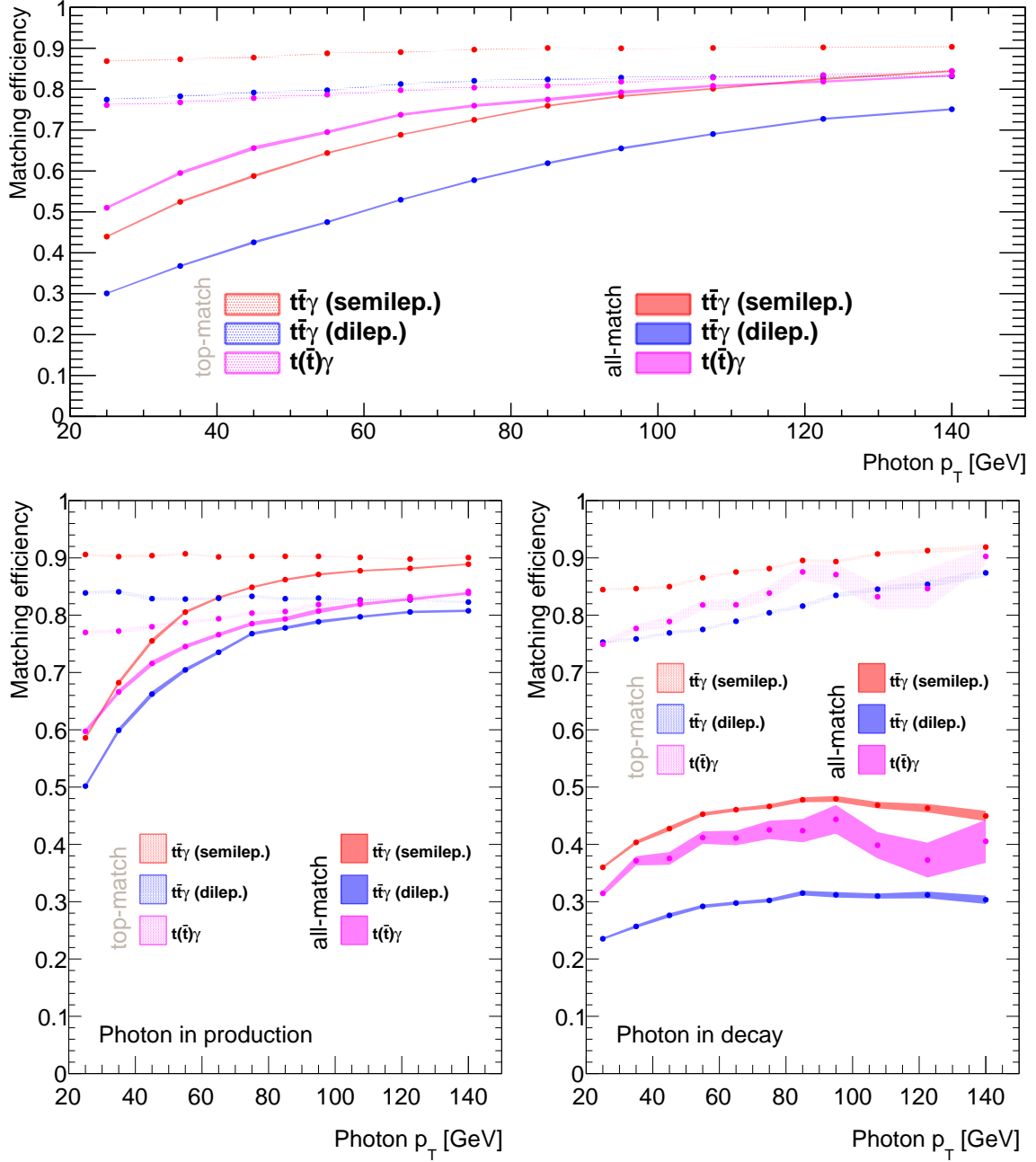


Figure 4. Efficiency of correct assignment between parton- and reco-level objects in top quark events with photon emission (top), as well as in events where a photon is radiated either in the production process (bottom left) or in a decay of a top quark (bottom right). The efficiencies are shown at central values of bins defined in the photon p_T and are presented for the correct matching of the decay products of the produced top quarks (“top-match”) and when, in addition, the photon is required to be correctly identified (“all-match”). Colored bands represent the statistical uncertainty.

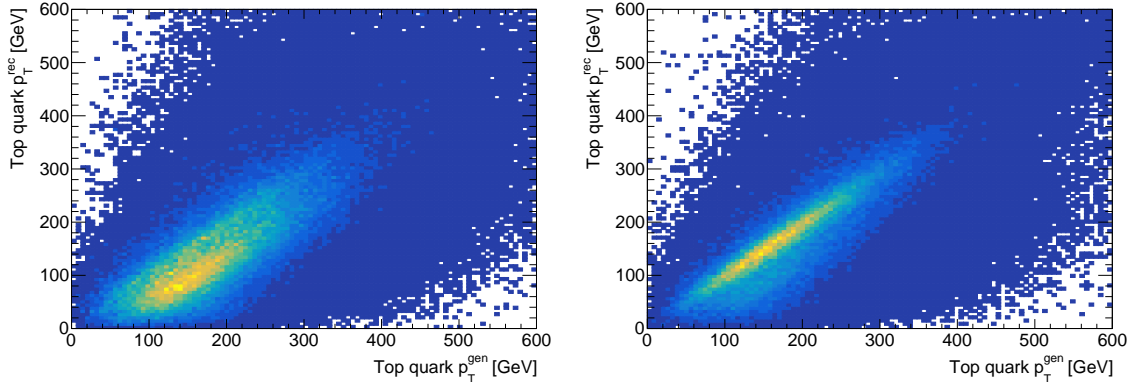


Figure 5. Transverse momentum of the top quark that corresponds to a W boson leptonic decay as obtained in semileptonic $t\bar{t}\gamma$ events with a radiated photon of $p_T > 50$ GeV. A correlation pattern is shown between the generated and the reconstructed values, when excluding (left) or including (right) the reconstructed photon in the kinematic fit.

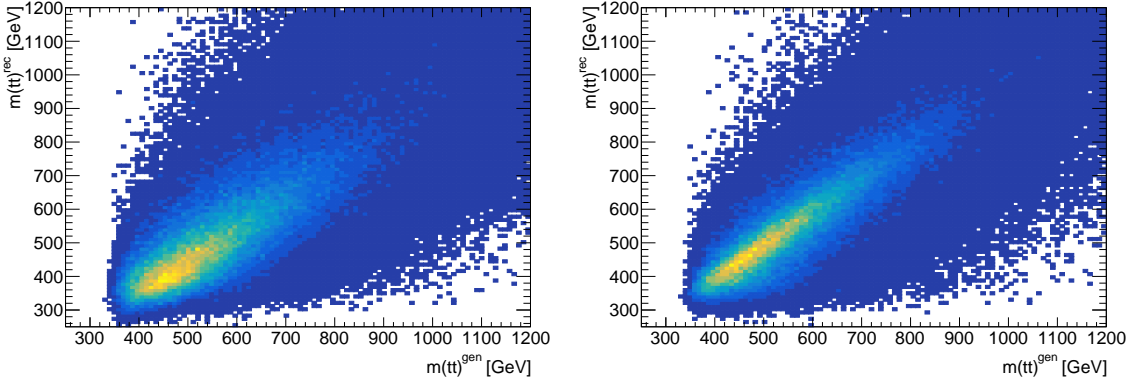


Figure 6. Invariant mass of two top quarks in semileptonic $t\bar{t}\gamma$ events with a radiated photon of $p_T > 50$ GeV. A correlation pattern is shown between the generated and the reconstructed values, when excluding (left) or including (right) the reconstructed photon in the kinematic fit.

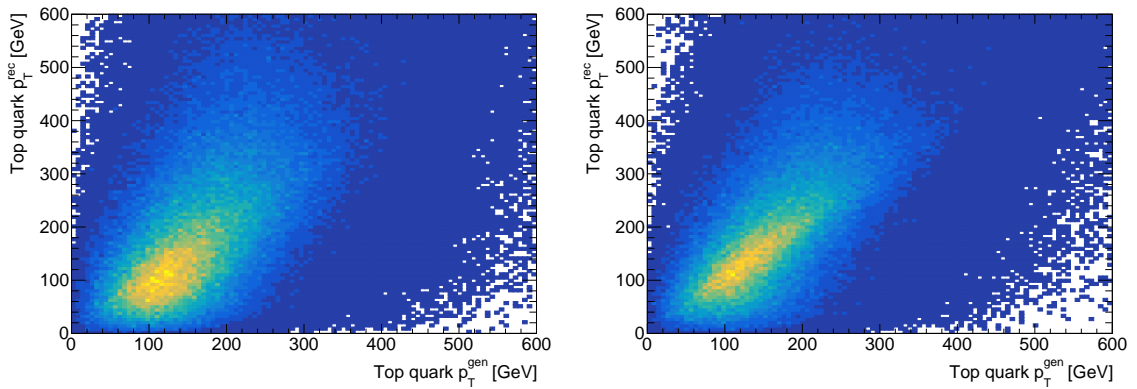


Figure 7. Transverse momentum of top quarks in dilepton $t\bar{t}\gamma$ events with a radiated photon of $p_T > 50$ GeV. A correlation pattern is shown between the generated and the reconstructed values, when excluding (left) or including (right) the reconstructed photon in the kinematic fit.

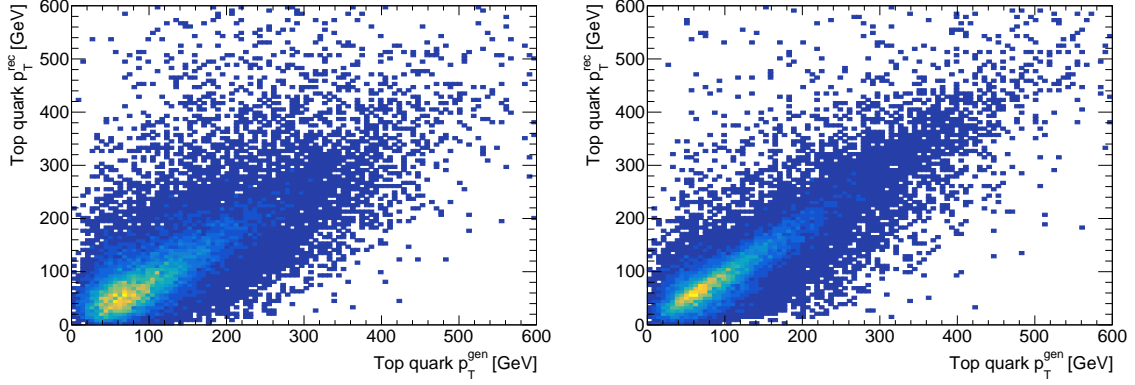


Figure 8. Transverse momentum of top quarks in $t(\bar{t})\gamma$ events with a radiated photon of $p_T > 20$ GeV. A correlation pattern is shown between the generated and the reconstructed values, when excluding (left) or including (right) the reconstructed photon in the kinematic fit.

precision of the differential cross section measurements, especially in the low photon p_T region, as well as at providing an additional handle for the top quark charge asymmetry measurement. The presented algorithm of kinematic reconstruction only relies on the knowledge of the top quark and the W boson masses and therefore can be applied to other processes with similar decay topologies where photon radiation effects are of importance.

Acknowledgments

We would like to warmly thank Dennis Schwarz, Francisco Yumiceva, Nadjieh Jafari and Daniel Noonan for carefully reading the manuscript and for providing an invaluable set of comments on the presented study. We also thank Robert Schöfbeck and Lukas Lechner for numerous discussions on the subject of an experimental study of the process with the production of top quark pairs in association with photons over the past years.

References

- [1] G. Aad et al. (ATLAS Collaboration), *Measurement of the $t\bar{t}$ production cross-section and lepton differential distributions in $e\mu$ dilepton events from pp collisions at $\sqrt{s} = 13$ TeV with the ATLAS detector*, *Eur. Phys. J. C* **80** (2020) 528 [arXiv:1910.08819].
- [2] A. M. Sirunyan et al. (CMS Collaboration), *Measurement of the single top quark and antiquark production cross sections in the t channel and their ratio in proton-proton collisions at $\sqrt{s} = 13$ TeV*, *Phys. Lett. B* **800** (2019) 135042 [arXiv:1812.10514].
- [3] U. Baur, M. Buice and L. H. Orr, *Direct measurement of the top quark charge at hadron colliders*, *Phys. Rev. D* **64** (2001) 094019 [arXiv:hep-ph/0106341].
- [4] U. Baur, M. Buice, L. H. Orr and D. Rainwater, *Probing electroweak top quark couplings at hadron colliders*, *Phys. Rev. D* **71** (2005) 054013 [arXiv:hep-ph/0412021].
- [5] G. Bevilacqua, H. B. Hartanto, M. Kraus, T. Weber, and M. Worek, *Off-shell vs on-shell modelling of top quarks in photon associated production*, *JHEP* **03** (2020) 154 [arXiv:1912.09999].

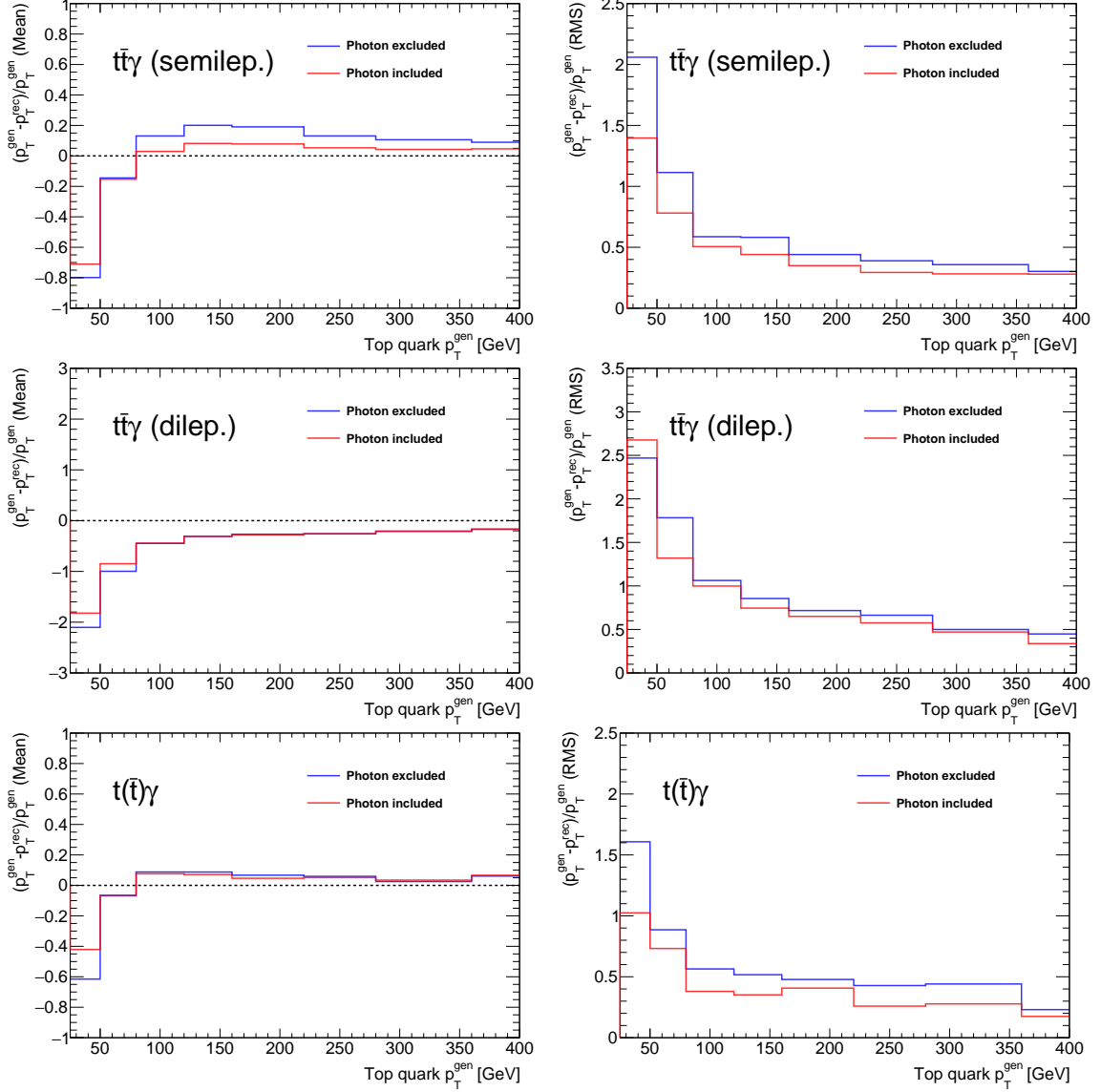


Figure 9. The measured mean values and the corresponding variances for the relative difference in the transverse momentum of reconstructed and generated top quarks in semileptonic $t\bar{t}\gamma$, dilepton $t\bar{t}\gamma$ and $t(\bar{t})\gamma$ events. The comparison is presented for two scenarios: when a radiated photon of $p_T > 50$ (20) GeV in $t\bar{t}\gamma$ ($t(\bar{t})\gamma$) events is either excluded or included in the kinematic fit.

- [6] G. Bevilacqua, H. B. Hartanto, M. Kraus, T. Weber, and M. Worek, *Hard photons in hadroproduction of top quarks with realistic final states*, *JHEP* **10** (2018) 158 [arXiv:1803.09916].
- [7] G. Bevilacqua, H. B. Hartanto, M. Kraus, T. Weber, and M. Worek, *Precise predictions for $t\bar{t}\gamma/t\bar{t}$ cross section ratios at the LHC*, *JHEP* **01** (2019) 188 [arXiv:1809.08562].
- [8] D. Pagani, H.-S. Shao, I. Tsinikos and M. Zaro, *Automated EW corrections with isolated photons: $t\bar{t}\gamma$, $t\bar{t}\gamma\gamma$ and $t\gamma j$ as case studies*, arXiv:2106.02059.
- [9] J. Bergner and M. Schulze, *The top quark charge asymmetry in $t\bar{t}\gamma$ production at the LHC*, *Eur. Phys. J. C* **79** (2019) 189 [arXiv:1812.10535].

- [10] J. A. Aguilar-Saavedra, *A Minimal set of top anomalous couplings*, *Nucl. Phys. B* **812** (2009) 181 [arXiv:0811.3842].
- [11] A. O. Bouzas and F. Larios, *Electromagnetic dipole moments of the top quark*, *Phys. Rev. D* **87** (2013) 074015 [arXiv:1212.6575].
- [12] J. A. Aguilar Saavedra et al., *Interpreting top-quark LHC measurements in the standard-model effective field theory*, arXiv:1802.07237.
- [13] T. Aaltonen et al. (CDF Collaboration), *Evidence for $t\bar{t}\gamma$ production and measurement of $\sigma_{t\bar{t}\gamma}/\sigma_{t\bar{t}}$* , *Phys. Rev. D* **84** (2011) 031104 [arXiv:1106.3970].
- [14] G. Aad et al. (ATLAS Collaboration), *Observation of top-quark pair production in association with a photon and measurement of the $t\bar{t}\gamma$ production cross section in pp collisions at $\sqrt{s} = 7$ TeV using the ATLAS detector*, *Phys. Rev. D* **91** (2015) 072007 [arXiv:1502.00586].
- [15] M. Aaboud et al. (ATLAS Collaboration), *Measurement of the $t\bar{t}\gamma$ production cross section in proton-proton collisions at $\sqrt{s} = 8$ TeV with the ATLAS detector*, *JHEP* **11** (2017) 086 [arXiv:1706.03046].
- [16] M. Aaboud et al. (ATLAS Collaboration), *Measurements of inclusive and differential fiducial cross-sections of $t\bar{t}\gamma$ in leptonic final states in pp collisions at $\sqrt{s} = 13$ TeV in ATLAS*, *Eur. Phys. J. C* **79** (2019) 382 [arXiv:1812.01697].
- [17] M. Aaboud et al. (ATLAS Collaboration), *Measurements of inclusive and differential cross-sections of combined $t\bar{t}\gamma$ and $tW\gamma$ production in the $e\mu$ channel at 13 TeV with the ATLAS detector*, *JHEP* **09** (2020) 049 [arXiv:2007.06946].
- [18] A. M. Sirunyan et al. (CMS Collaboration), *Measurement of the semileptonic $t\bar{t}+\gamma$ production cross section in pp collisions at $\sqrt{s} = 8$ TeV*, *JHEP* **10** (2017) 006 [arXiv:1706.08128].
- [19] A. M. Sirunyan et al. (CMS Collaboration), *Measurement of the inclusive and differential $t\bar{t}+\gamma$ cross section and EFT interpretation in the single lepton channel at $\sqrt{s} = 13$ TeV*, arXiv:2107.01508.
- [20] M. Fael and T. Gehrmann, *Probing top quark electromagnetic dipole moments in single-top-plus-photon production*, *Phys. Rev. D* **88** (2013) 033003 [arXiv:1307.1349].
- [21] S. M. Etesami, S. Khatibi, and M. Mohammadi Najafabadi, *Measuring anomalous $WW\gamma$ and $t\bar{t}\gamma$ couplings using $top+\gamma$ production at the LHC*, *Eur. Phys. J. C* **76** (2016) 533 [arXiv:1606.02178].
- [22] A. M. Sirunyan et al. (CMS Collaboration), *Evidence for the associated production of a single top quark and a photon in proton-proton collisions at $\sqrt{s} = 13$ TeV*, *Phys. Rev. Lett.* **121** (2018) 221802 [arXiv:1808.02913].
- [23] J. Alwall et al., *The automated computation of tree-level and next-to-leading order differential cross sections, and their matching to parton shower simulations*, *JHEP* **07** (2014) 079 [arXiv:1405.0301].
- [24] T. Sjöstrand, S. Mrenna and P. Skands, *The automated computation of tree-level and next-to-leading order differential cross sections, and their matching to parton shower simulations*, *JHEP* **05** (2006) 026 [arXiv:hep-ph/0603175], *Comput. Phys. Comm.* **178** (2008) 852 [arXiv:0710.3820].
- [25] J. de Favereau et al., *DELPHES 3, A modular framework for fast simulation of a generic collider experiment*, *JHEP* **02** (2014) 057 [arXiv:1307.6346].
- [26] M. Cacciari, G. P. Salam and G. Soyez, *The anti- k_T jet clustering algorithm*, *JHEP* **04** (2008) 063 [arXiv:0802.1189].
- [27] B. Abbott et al. (D0 Collaboration), *Measurement of the top quark mass in the dilepton channel*, *Phys. Rev. D* **60** (1999) 052001 [arXiv:hep-ex/9808029].

- [28] A. Abulencia et al. (CDF Collaboration), *Measurement of the top quark mass using template methods on dilepton events in $p\bar{p}$ collisions at $\sqrt{s} = 1.96$ TeV*, *Phys. Rev. D* **73** (2006) 112006 [[arXiv:hep-ex/0602008](#)].
- [29] V.M. Abazov et al. (D0 Collaboration), *Precise measurement of the top quark mass in dilepton decays using optimized neutrino weighting*, *Phys. Lett. B* **752** (2016) 18 [[arXiv:1508.03322](#)].
- [30] S. Chatrchyan et al. (CMS Collaboration), *Measurement of the top-quark mass in $t\bar{t}$ events with dilepton final states in pp collisions at $\sqrt{s} = 7$ TeV*, *Eur. Phys. J. C* **72** (2012) 2202 [[arXiv:1209.2393](#)].
- [31] J. Erdmann et al., *A likelihood-based reconstruction algorithm for top-quark pairs and the KLFitter framework*, *Nucl. Instrum. Meth. A* **748** (2014) 18 [[arXiv:1312.5595](#)].
- [32] J. Erdmann et al., *From the Bottom to the Top – Reconstruction of $t\bar{t}$ events with deep learning*, *JINST* **14** (2019) P11015 [[arXiv:1907.11181](#)].
- [33] H. Casler, M. Manganel, M. Fiolhais, A. Ferroglia, and A. Onofre, *Reconstruction of top quark pair dilepton decays in electron-positron collisions*, *Phys. Rev. D* **99** (2019) 054011 [[arXiv:1902.01976](#)].
- [34] J. Kvita, *Study of methods of resolved top quark reconstruction in semileptonic $t\bar{t}$ decay*, *Nucl. Instrum. Meth. A* **900** (2018) 84 [[arXiv:1806.05463](#)].
- [35] F. Syed, R. Di Sipio, P. Sinervo, *Bidirectional Long Short-Term Memory (BLSTM) neural networks for reconstruction of top-quark pair decay kinematics*, [arXiv:1909.01144](#).
- [36] B. A. Betchart, R. Demina, A. Harel, *Analytic solutions for neutrino momenta in decay of top quarks*, *Nucl. Instrum. Meth. A* **736** (2014) 169 [[arXiv:1305.1878](#)].
- [37] R. Demina, A. Harel, D. Orbaker, *Reconstructing top quark-antiquark events with one lost jet*, *Nucl. Instrum. Meth. A* **788** (2015) 128 [[arXiv:1310.3263](#)].
- [38] L. Sonnenschein, *Algebraic approach to solve $t\bar{t}$ dilepton equations*, *Phys. Rev. D* **72** (2005) 095020 [[arXiv:hep-ph/0510100](#)].
- [39] <https://github.com/kskovpen/TopPhit>
- [40] R. Brun and F. Rademakers, *ROOT - An object oriented data analysis framework*, *Nucl. Instrum. Meth. A* **389** (1997) 81.
- [41] F. James and M. Roos, *Minuit: A System for Function Minimization and Analysis of the Parameter Errors and Correlations*, *Comput. Phys. Commun.* **10** (1975) 343.